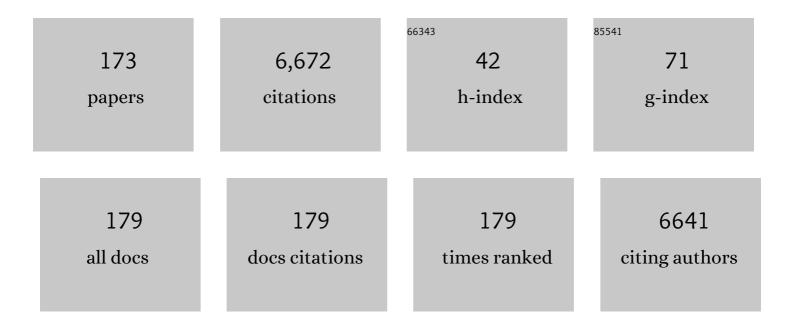
List of Publications by Year in descending order

Source: https://exaly.com/author-pdf/5629483/publications.pdf Version: 2024-02-01



YIVUN HUANC

#	Article	IF	CITATIONS
1	Feasibility study of PET dynamic imaging of [18F]DHMT for quantification of reactive oxygen species in the myocardium of large animals. Journal of Nuclear Cardiology, 2022, 29, 216-225.	2.1	5
2	Imaging Pituitary Vasopressin 1B Receptor in Humans with the PET Radiotracer <sup>11</sup> C-TASP699. Journal of Nuclear Medicine, 2022, 63, 609-614.	5.0	7
3	Discovery and development of brain-penetrant 18F-labeled radioligands for neuroimaging of the sigma-2 receptors. Acta Pharmaceutica Sinica B, 2022, 12, 1406-1415.	12.0	6
4	Recently Abstinent Smokers Exhibit Mood-Associated Dopamine Dysfunction in the Ventral Striatum Compared to Nonsmokers: A [11C]-(+)-PHNO PET Study. Nicotine and Tobacco Research, 2022, 24, 745-752.	2.6	5
5	Association of entorhinal cortical tau deposition and hippocampal synaptic density in older individuals with normal cognition and early Alzheimer's disease. Neurobiology of Aging, 2022, 111, 44-53.	3.1	25
6	A metabolically stable PET tracer for imaging synaptic vesicle protein 2A: synthesis and preclinical characterization of [18F]SDM-16. European Journal of Nuclear Medicine and Molecular Imaging, 2022, 49, 1482-1496.	6.4	16
7	Lower prefrontal cortical synaptic vesicle binding in cocaine use disorder: An exploratory <sup>11</sup> Câ€UCBâ€J positron emission tomography study in humans. Addiction Biology, 2022, 27, e13123.	2.6	16
8	Cortical abnormalities of synaptic vesicle protein 2A in focal cortical dysplasia type II identified in vivo with 18F-SynVesT-1 positron emission tomography imaging. European Journal of Nuclear Medicine and Molecular Imaging, 2022, 49, 3482-3491.	6.4	11
9	Translational PET Imaging of Spinal Cord Injury with the Serotonin Transporter Tracer [11C]AFM. Molecular Imaging and Biology, 2022, , 1.	2.6	0
10	Characterization in nonhuman primates of (R)-[18F]OF-Me-NB1 and (S)-[18F]OF-Me-NB1 for imaging the GluN2B subunits of the NMDA receptor. European Journal of Nuclear Medicine and Molecular Imaging, 2022, , 1.	6.4	8
11	Comparison of three novel radiotracers for CluN2B-containing NMDA receptors in non-human primates: <i>(R)</i> -[ <sup>11</sup> C]NR2B-Me, <i>(R)</i> -[ <sup>18</sup> F]of-Me-NB1, and <i>(S)</i> -[ <sup>18</sup> F]of-NB1. Journal of Cerebral Blood Flow and Metabolism, 2022, 42, 1398-1409.	4.3	7
12	Synaptic density and cognitive performance in Alzheimer's disease: A PET imaging study with [ <sup>11</sup> C]UCBâ€J. Alzheimer's and Dementia, 2022, 18, 2527-2536.	0.8	55
13	Synthesis and characterization of the two enantiomers of a chiral sigma-1 receptor radioligand: (S)-(+)- and (R)-(-)-[18F]FBFP. Chinese Chemical Letters, 2022, 33, 3543-3548.	9.0	6
14	Feasibility of imaging synaptic density in the human spinal cord using [11C]UCB-J PET. EJNMMI Physics, 2022, 9, 32.	2.7	3
15	PET Imaging in Animal Models of Alzheimer's Disease. Frontiers in Neuroscience, 2022, 16, .	2.8	4
16	Differences in the association between kappa opioid receptors and pain among Black and White adults with alcohol use disorders. Alcoholism: Clinical and Experimental Research, 2022, 46, 1348-1357.	2.4	2
17	Imaging the fetal nonhuman primate brain with SV2A positron emission tomography (PET). European Journal of Nuclear Medicine and Molecular Imaging, 2022, 49, 3679-3691.	6.4	4
18	Preliminary in vivo evidence of lower hippocampal synaptic density in cannabis use disorder. Molecular Psychiatry, 2021, 26, 3192-3200.	7.9	32

#	Article	IF	CITATIONS
19	Occupancy of the kappa opioid receptor by naltrexone predicts reduction in drinking and craving. Molecular Psychiatry, 2021, 26, 5053-5060.	7.9	17
20	Development of [89Zr]ZrDFO-amivantamab bispecific to EGFR and c-MET for PET imaging of triple-negative breast cancer. European Journal of Nuclear Medicine and Molecular Imaging, 2021, 48, 383-394.	6.4	20
21	Binding of the synaptic vesicle radiotracer [ <sup>11</sup> C]UCB-J is unchanged during functional brain activation using a visual stimulation task. Journal of Cerebral Blood Flow and Metabolism, 2021, 41, 1067-1079.	4.3	28
22	Simplified Quantification of <sup>11</sup> C-UCB-J PET Evaluated in a Large Human Cohort. Journal of Nuclear Medicine, 2021, 62, 418-421.	5.0	19
23	First-in-Human Evaluation of <sup>18</sup> F-SynVesT-1, a Radioligand for PET Imaging of Synaptic Vesicle Glycoprotein 2A. Journal of Nuclear Medicine, 2021, 62, 561-567.	5.0	60
24	Quantification of SV2A Binding in Rodent Brain Using [18F]SynVesT-1 and PET Imaging. Molecular Imaging and Biology, 2021, 23, 372-381.	2.6	20
25	First-in-Human Assessment of <sup>11</sup> C-LSN3172176, an M1 Muscarinic Acetylcholine Receptor PET Radiotracer. Journal of Nuclear Medicine, 2021, 62, 553-560.	5.0	35
26	PET Imaging Estimates of Regional Acetylcholine Concentration Variation in Living Human Brain. Cerebral Cortex, 2021, 31, 2787-2798.	2.9	5
27	Association of Aβ deposition and regional synaptic density in early Alzheimer's disease: a PET imaging study with [11C]UCB-J. Alzheimer's Research and Therapy, 2021, 13, 11.	6.2	53
28	Assessment of test-retest reproducibility of [18F]SynVesT-1, a novel radiotracer for PET imaging of synaptic vesicle glycoprotein 2A. European Journal of Nuclear Medicine and Molecular Imaging, 2021, 48, 1327-1338.	6.4	23
29	Dopamine D2/3 receptor availability in cocaine use disorder individuals with obesity as measured by [11C]PHNO PET. Drug and Alcohol Dependence, 2021, 220, 108514.	3.2	1
30	Comparison of [ <sup>11</sup> C]UCB-J and [ <sup>18</sup> F]FDG PET in Alzheimer's disease: A tracer kinetic modeling study. Journal of Cerebral Blood Flow and Metabolism, 2021, 41, 2395-2409.	4.3	43
31	Preclinical Advances in Theranostics for the Different Molecular Subtypes of Breast Cancer. Frontiers in Pharmacology, 2021, 12, 627693.	3.5	10
32	Preliminary In Vivo Evidence of Reduced Synaptic Density in Human Immunodeficiency Virus (HIV) Despite Antiretroviral Therapy. Clinical Infectious Diseases, 2021, 73, 1404-1411.	5.8	25
33	Social Rank, Behavioral Phenotypes and Kappa Opioid Receptor: PET Imaging Studies of Socially Housed Female and Male Monkey Models of Cocaine Use Disorder. FASEB Journal, 2021, 35, .	0.5	Ο
34	In vivo evidence of lower synaptic vesicle density in schizophrenia. Molecular Psychiatry, 2021, 26, 7690-7698.	7.9	51
35	Effect of age on brain metabotropic glutamate receptor subtype 5 measured with [18F]FPEB PET. NeuroImage, 2021, 238, 118217.	4.2	10
36	Imaging brain cortisol regulation in PTSD with a target for 11β-hydroxysteroid dehydrogenase type 1. Journal of Clinical Investigation, 2021, 131, .	8.2	10

#	Article	IF	CITATIONS
37	Further Investigation of Synaptic Vesicle Protein 2A (SV2A) Ligands Designed for Positron Emission Tomography and Single-Photon Emission Computed Tomography Imaging: Synthesis and Structure–Activity Relationship of Substituted Pyridinylmethyl-4-(3,5-difluorophenyl)pyrrolidin-2-ones. ACS Omega, 2021, 6, 27676-27683.	3.5	2
38	Validation of SV2A-Targeted PET Imaging for Noninvasive Assessment of Neuroendocrine Differentiation in Prostate Cancer. International Journal of Molecular Sciences, 2021, 22, 13085.	4.1	10
39	First in-human PET study and kinetic evaluation of [ <sup>18</sup> F]AS2471907 for imaging 11β-hydroxysteroid dehydrogenase type 1. Journal of Cerebral Blood Flow and Metabolism, 2020, 40, 695-704.	4.3	10
40	PET Imaging of Pancreatic Dopamine D <sub>2</sub> and D <sub>3</sub> Receptor Density with <sup>11</sup> C-(+)-PHNO in Type 1 Diabetes. Journal of Nuclear Medicine, 2020, 61, 570-576.	5.0	19
41	Preclinical In Vitro and In Vivo Characterization of Synaptic Vesicle 2A–Targeting Compounds Amenable to F-18 Labeling as Potential PET Radioligands for Imaging of Synapse Integrity. Molecular Imaging and Biology, 2020, 22, 832-841.	2.6	23
42	Assessment of a white matter reference region for <sup>11</sup> C-UCB-J PET quantification. Journal of Cerebral Blood Flow and Metabolism, 2020, 40, 1890-1901.	4.3	77
43	In vivo 5-HT6 and 5-HT2A receptor availability in antipsychotic treated schizophrenia patients vs. unmedicated healthy humans measured with [11C]GSK215083 PET. Psychiatry Research - Neuroimaging, 2020, 295, 111007.	1.8	17
44	Reduced synaptic vesicle protein 2A binding in temporal lobe epilepsy: A [ <sup>11</sup> C]UCBâ€J positron emission tomography study. Epilepsia, 2020, 61, 2183-2193.	5.1	51
45	In vivo measurement of widespread synaptic loss and associated tau accumulation in early Alzheimer's disease. Alzheimer's and Dementia, 2020, 16, e037791.	0.8	1
46	PBR28 Brain PET imaging with lipopolysaccharide challenge for the study of microglia function in Alzheimer's disease. Alzheimer's and Dementia, 2020, 16, e037792.	0.8	0
47	11Câ€PBR28 brain PET imaging with lipopolysaccharide challenge for the study of microglia function in Alzheimer's disease. Alzheimer's and Dementia, 2020, 16, e043584.	0.8	0
48	Association between cerebral amyloid accumulation and synaptic density in Alzheimer's disease: A multitracer PET study. Alzheimer's and Dementia, 2020, 16, e043631.	0.8	0
49	Association between cerebrospinal fluid biomarkers of neurodegeneration and PET measurements of synaptic density in Alzheimer's disease. Alzheimer's and Dementia, 2020, 16, e044211.	0.8	2
50	Validation of a simplified tissueâ€ŧoâ€ŧeference ratio measurement using SUVR for the assessment of synaptic density alterations in Alzheimer's disease using [ 11 C]UCBâ€J PET. Alzheimer's and Dementia, 2020, 16, e045928.	0.8	1
51	In vivo measurement of widespread synaptic loss in Alzheimer's disease with SV2A PET. Alzheimer's and Dementia, 2020, 16, 974-982.	0.8	170
52	PTSD is associated with neuroimmune suppression: evidence from PET imaging and postmortem transcriptomic studies. Nature Communications, 2020, 11, 2360.	12.8	56
53	Body Mass Index and Age Effects on Brain 11β-Hydroxysteroid Dehydrogenase Type 1: a Positron Emission Tomography Study. Molecular Imaging and Biology, 2020, 22, 1124-1131.	2.6	9
54	Synthesis and Preclinical Evaluation of an <sup>18</sup> F-Labeled Synaptic Vesicle Glycoprotein 2A PET Imaging Probe: [ <sup>18</sup> F]SynVesT-2. ACS Chemical Neuroscience, 2020, 11, 592-603.	3.5	34

#	Article	IF	CITATIONS
55	Synaptic Changes in Parkinson Disease Assessed with in vivo Imaging. Annals of Neurology, 2020, 87, 329-338.	5.3	112
56	PET imaging of mCluR5 in Alzheimer's disease. Alzheimer's Research and Therapy, 2020, 12, 15.	6.2	29
57	Tobacco Smoking in People Is Not Associated with Altered 18-kDa Translocator Protein Levels: A PET Study. Journal of Nuclear Medicine, 2020, 61, 1200-1204.	5.0	8
58	Inverse changes in raphe and cortical 5â€HT 1B receptor availability after acute tryptophan depletion in healthy human subjects. Synapse, 2020, 74, e22159.	1.2	9
59	Positron Emission Tomography Imaging Evaluation of a Novel 18F-Labeled Sigma-1 Receptor Radioligand in Cynomolgus Monkeys. ACS Chemical Neuroscience, 2020, 11, 1673-1681.	3.5	10
60	Separating dopamine D2 and D3 receptor sources of [11C]-(+)-PHNO binding potential: Independent component analysis of competitive binding. NeuroImage, 2020, 214, 116762.	4.2	9
61	Synthesis and evaluation of new 1-oxa-8-azaspiro[4.5]decane derivatives as candidate radioligands for sigma-1 receptors. Bioorganic and Medicinal Chemistry, 2020, 28, 115560.	3.0	6
62	Human adult and adolescent biodistribution and dosimetry of the synaptic vesicle glycoprotein 2A radioligand 11C-UCB-J. EJNMMI Research, 2020, 10, 83.	2.5	8
63	Imaging sigma receptors in the brain: New opportunities for diagnosis of Alzheimer's disease and therapeutic development. Neuroscience Letters, 2019, 691, 3-10.	2.1	24
64	PET imaging of synaptic density: A new tool for investigation of neuropsychiatric diseases. Neuroscience Letters, 2019, 691, 44-50.	2.1	85
65	The Kappa Opioid Receptor Is Associated With Naltrexone-Induced Reduction of Drinking and Craving. Biological Psychiatry, 2019, 86, 864-871.	1.3	27
66	Anti-edema and antioxidant combination therapy for ischemic stroke via glyburide-loaded betulinic acid nanoparticles. Theranostics, 2019, 9, 6991-7002.	10.0	54
67	A Novel <sup>18</sup> F-Labeled Radioligand for Positron Emission Tomography Imaging of 11β-Hydroxysteroid Dehydrogenase (11I²-HSD1): Synthesis and Preliminary Evaluation in Nonhuman Primates. ACS Chemical Neuroscience, 2019, 10, 2450-2458.	3.5	12
68	Synthesis and in vivo evaluation of [18F]UCB-J for PET imaging of synaptic vesicle glycoprotein 2A (SV2A). European Journal of Nuclear Medicine and Molecular Imaging, 2019, 46, 1952-1965.	6.4	38
69	In Vivo Synaptic Density Imaging with <sup>11</sup> C-UCB-J Detects Treatment Effects of Saracatinib in a Mouse Model of Alzheimer Disease. Journal of Nuclear Medicine, 2019, 60, 1780-1786.	5.0	57
70	Kappa-opioid receptors, dynorphin, and cocaine addiction: a positron emission tomography study. Neuropsychopharmacology, 2019, 44, 1720-1727.	5.4	36
71	<sup>18</sup> F‣abeled benzylpiperazine derivatives as highly selective ligands for imaging Ïf <sub>1</sub> receptor with positron emission tomography. Journal of Labelled Compounds and Radiopharmaceuticals, 2019, 62, 425-437.	1.0	2
72	Imaging the Enzyme 11β-Hydroxysteroid Dehydrogenase Type 1 with PET: Evaluation of the Novel Radiotracer <sup>11</sup> C-AS2471907 in Human Brain. Journal of Nuclear Medicine, 2019, 60, 1140-1146.	5.0	11

#	Article	IF	CITATIONS
73	Social status and demographic effects of the kappa opioid receptor: a PET imaging study with a novel agonist radiotracer in healthy volunteers. Neuropsychopharmacology, 2019, 44, 1714-1719.	5.4	22
74	A singleâ€center, openâ€label positron emission tomography study to evaluate brivaracetam and levetiracetam synaptic vesicle glycoprotein 2A binding in healthy volunteers. Epilepsia, 2019, 60, 958-967.	5.1	45
75	Evaluation of <sup>11</sup> C-LSN3172176 as a Novel PET Tracer for Imaging M <sub>1</sub> Muscarinic Acetylcholine Receptors in Nonhuman Primates. Journal of Nuclear Medicine, 2019, 60, 1147-1153.	5.0	17
76	Novel Kappa Opioid Receptor Agonist as Improved PET Radiotracer: Development and in Vivo Evaluation. Molecular Pharmaceutics, 2019, 16, 1523-1531.	4.6	9
77	P4â€481: ASSOCIATION BETWEEN ENTORHINAL CORTICAL TAU ACCUMULATION AND HIPPOCAMPAL SYNAPTIC DENSITY IN OLDER INDIVIDUALS WITH NORMAL COGNITION AND EARLY ALZHEIMER'S DISEASE: PRELIMINARY EXPERIENCE. Alzheimer's and Dementia, 2019, 15, P1497.	0.8	0
78	ICâ€Pâ€140: ASSOCIATION BETWEEN MGLUR5 AND SYNAPTIC DENSITY: A MULTIâ€TRACER STUDY IN HEALTHY / AND ALZHEIMER'S DISEASE. Alzheimer's and Dementia, 2019, 15, P115.	AGING	0
79	Binge alcohol use is not associated with alterations in striatal dopamine receptor binding or dopamine release. Drug and Alcohol Dependence, 2019, 205, 107627.	3.2	7
80	Synthesis and <i>in Vivo</i> Evaluation of a Novel PET Radiotracer for Imaging of Synaptic Vesicle Glycoprotein 2A (SV2A) in Nonhuman Primates. ACS Chemical Neuroscience, 2019, 10, 1544-1554.	3.5	70
81	Quantification of Positron Emission Tomography Data Using Simultaneous Estimation of the Input Function: Validation with Venous Blood and Replication of Clinical Studies. Molecular Imaging and Biology, 2019, 21, 926-934.	2.6	16
82	Development and In Vivo Evaluation of a κ-Opioid Receptor Agonist as a PET Radiotracer with Superior Imaging Characteristics. Journal of Nuclear Medicine, 2019, 60, 1023-1030.	5.0	20
83	Age-Related Change in 5-HT <sub>6</sub> Receptor Availability in Healthy Male Volunteers Measured with <sup>11</sup> C-GSK215083 PET. Journal of Nuclear Medicine, 2018, 59, 1445-1450.	5.0	34
84	Evaluation of PET Brain Radioligands for Imaging Pancreatic β-Cell Mass: Potential Utility of 11C-(+)-PHNO. Journal of Nuclear Medicine, 2018, 59, 1249-1254.	5.0	22
85	Novel <sup>18</sup> F-Labeled κ-Opioid Receptor Antagonist as PET Radiotracer: Synthesis and In Vivo Evaluation of <sup>18</sup> F-LY2459989 in Nonhuman Primates. Journal of Nuclear Medicine, 2018, 59, 140-146.	5.0	28
86	The Effect of Treatment with Guanfacine, an Alpha2 Adrenergic Agonist, on Dopaminergic Tone in Tobacco Smokers: An [11C]FLB457 PET Study. Neuropsychopharmacology, 2018, 43, 1052-1058.	5.4	12
87	Evaluation of the Lysophosphatidic Acid Receptor Type 1 Radioligand <sup>11</sup> C-BMT-136088 for Lung Imaging in Rhesus Monkeys. Journal of Nuclear Medicine, 2018, 59, 327-333.	5.0	16
88	Cortical β-amyloid burden, gray matter, and memory in adults at varying APOE ε4 risk for Alzheimer's disease. Neurobiology of Aging, 2018, 61, 207-214.	3.1	28
89	Evaluation of (â€)â€{ <sup>18</sup> <scp>F]F</scp> lubatineâ€specific binding: Implications for reference region approaches. Synapse, 2018, 72, e22016.	1.2	7
90	Kinetic evaluation and test–retest reproducibility of [ <sup>11</sup> C]UCB-J, a novel radioligand for positron emission tomography imaging of synaptic vesicle glycoprotein 2A in humans. Journal of Cerebral Blood Flow and Metabolism, 2018, 38, 2041-2052.	4.3	143

#	Article	IF	CITATIONS
91	P2â€365: PET IMAGING OF SYNAPTIC DENSITY (SYNAPTIC VESICLE GLYCOPROTEIN 2A, SV2A) IN ALZHEIMER'S DISEASE: INITIAL EXPERIENCE. Alzheimer's and Dementia, 2018, 14, P832.	0.8	0
92	ICâ€Pâ€183: PET IMAGING OF SYNAPTIC DENSITY (SYNAPTIC VESICLE GLYCOPROTEIN 2A, SV2A) IN ALZHEIMER'S DISEASE: INITIAL EXPERIENCE. Alzheimer's and Dementia, 2018, 14, P152.	0.8	0
93	PET imaging reveals lower kappa opioid receptor availability in alcoholics but no effect of age. Neuropsychopharmacology, 2018, 43, 2539-2547.	5.4	37
94	InÂVivo Reactive Oxygen Species Detection With a Novel Positron Emission Tomography Tracer, 18F-DHMT, Allows for Early Detection of Anthracycline-Induced Cardiotoxicity in Rodents. JACC Basic To Translational Science, 2018, 3, 378-390.	4.1	46
95	Bridging from Brain to Tumor Imaging: (S)-(â^')- and (R)-(+)-[18F]Fluspidine for Investigation of Sigma-1 Receptors in Tumor-Bearing Mice. Molecules, 2018, 23, 702.	3.8	9
96	Assessing Synaptic Density in Alzheimer Disease With Synaptic Vesicle Glycoprotein 2A Positron Emission Tomographic Imaging. JAMA Neurology, 2018, 75, 1215.	9.0	304
97	Protective and restorative effects of the traditional Chinese medicine Jitai tablet against methamphetamine-induced dopaminergic neurotoxicity. BMC Complementary and Alternative Medicine, 2018, 18, 76.	3.7	3
98	Automated radiosynthesis of [18F]FBEM, a sulfhydryl site specific labeling agent for peptides and proteins. Applied Radiation and Isotopes, 2018, 140, 294-299.	1.5	5
99	High Single Doses of Radiation May Induce Elevated Levels of Hypoxia in Early-Stage Non-Small Cell Lung Cancer Tumors. International Journal of Radiation Oncology Biology Physics, 2018, 102, 174-183.	0.8	36
100	A multi species evaluation of the radiation dosimetry of [ 11 C]erlotinib, the radiolabeled analog of a clinically utilized tyrosine kinase inhibitor. Nuclear Medicine and Biology, 2017, 47, 56-61.	0.6	8
101	PET Imaging Evaluation of Four Ïf <sub>1</sub> Radiotracers in Nonhuman Primates. Journal of Nuclear Medicine, 2017, 58, 982-988.	5.0	24
102	PET imaging of α7 nicotinic acetylcholine receptors: a comparative study of [18F]ASEM and [18F]DBT-10 in nonhuman primates, and further evaluation of [18F]ASEM in humans. European Journal of Nuclear Medicine and Molecular Imaging, 2017, 44, 1042-1050.	6.4	47
103	1-(4-[ <sup>18</sup> F]Fluorobenzyl)-4-[(tetrahydrofuran-2-yl)methyl]piperazine: A Novel Suitable Radioligand with Low Lipophilicity for Imaging σ <sub>1</sub> Receptors in the Brain. Journal of Medicinal Chemistry, 2017, 60, 4161-4172.	6.4	24
104	Quantification of Tumor Hypoxic Fractions Using Positron Emission Tomography with [18F]Fluoromisonidazole ([18F]FMISO) Kinetic Analysis and Invasive Oxygen Measurements. Molecular Imaging and Biology, 2017, 19, 893-902.	2.6	17
105	18 F-Labeled indole-based analogs as highly selective radioligands for imaging sigma-2 receptors in the brain. Bioorganic and Medicinal Chemistry, 2017, 25, 3792-3802.	3.0	18
106	PET Imaging for Early Detection of Alzheimer's Disease. PET Clinics, 2017, 12, 329-350.	3.0	44
107	A modification to improve the reliability of <scp>[<sup>11</sup>C]CN<sup>â^*</sup></scp> production in the <scp>GE</scp> radiochemistry system. Journal of Labelled Compounds and Radiopharmaceuticals, 2017, 60, 592-595.	1.0	5
108	The Search for a Subtype-Selective PET Imaging Agent for the GABA <sub>A</sub> Receptor Complex: Evaluation of the Radiotracer [ <sup>11</sup> C]ADO in Nonhuman Primates. Molecular Imaging, 2017, 16, 153601211773125.	1.4	8

#	Article	IF	CITATIONS
109	Fluorine-18-Labeled Antagonist for PET Imaging of Kappa Opioid Receptors. ACS Chemical Neuroscience, 2017, 8, 12-16.	3.5	23
110	Quantitative projection of human brain penetration of the H <sub>3</sub> antagonist PF-03654746 by integrating rat-derived brain partitioning and PET receptor occupancy. Xenobiotica, 2017, 47, 119-126.	1.1	5
111	Optimized and Automated Radiosynthesis of [18F]DHMT for Translational Imaging of Reactive Oxygen Species with Positron Emission Tomography. Molecules, 2016, 21, 1696.	3.8	18
112	Nicotine and Nicotine Abstinence Do Not Interfere with GABA <sub>A</sub> Receptor Neuroadaptations During Alcohol Abstinence. Alcoholism: Clinical and Experimental Research, 2016, 40, 698-705.	2.4	5
113	Comparative evaluation of two glycine transporter 1 radiotracers [11C]GSK931145 and [18F]MK-6577 in baboons. Synapse, 2016, 70, 112-120.	1.2	4
114	Preclinical Evaluation of <sup>18</sup> F-PF-05270430, a Novel PET Radioligand for the Phosphodiesterase 2A Enzyme. Journal of Nuclear Medicine, 2016, 57, 1448-1453.	5.0	13
115	Quantitative Analysis of Dynamic <sup>123</sup> I-mIBG SPECT Imaging Data in Healthy Humans with a Population-Based Metabolite Correction Method. Journal of Nuclear Medicine, 2016, 57, 1226-1232.	5.0	17
116	First-in-Human Assessment of the Novel PDE2A PET Radiotracer <sup>18</sup> F-PF-05270430. Journal of Nuclear Medicine, 2016, 57, 1388-1395.	5.0	27
117	Brivaracetam, a selective highâ€affinity synaptic vesicle protein 2A ( <scp>SV</scp> 2A) ligand with preclinical evidence of high brain permeability and fast onset of action. Epilepsia, 2016, 57, 201-209.	5.1	130
118	Preferential binding to dopamine D3 over D2 receptors by cariprazine in patients with schizophrenia using PET with the D3/D2 receptor ligand [11C]-(+)-PHNO. Psychopharmacology, 2016, 233, 3503-3512.	3.1	101
119	Imaging synaptic density in the living human brain. Science Translational Medicine, 2016, 8, 348ra96.	12.4	343
120	Age-related changes in binding of the D2/3 receptor radioligand [11C](+)PHNO in healthy volunteers. NeuroImage, 2016, 130, 241-247.	4.2	43
121	Receptor Occupancy of the Â-Opioid Antagonist LY2456302 Measured with Positron Emission Tomography and the Novel Radiotracer 11C-LY2795050. Journal of Pharmacology and Experimental Therapeutics, 2016, 356, 260-266.	2.5	47
122	Reduced Brain Cannabinoid Receptor Availability in Schizophrenia. Biological Psychiatry, 2016, 79, 997-1005.	1.3	83
123	Neuroprotective effects of stemazole in the MPTP-induced acute model of Parkinson's disease: Involvement of the dopamine system. Neuroscience Letters, 2016, 616, 152-159.	2.1	27
124	Rapid Changes in Cannabinoid 1 Receptor Availability in Cannabis-Dependent Male Subjects After Abstinence From Cannabis. Biological Psychiatry: Cognitive Neuroscience and Neuroimaging, 2016, 1, 60-67.	1.5	135
125	Synthesis and Preclinical Evaluation of <sup>11</sup> C-UCB-J as a PET Tracer for Imaging the Synaptic Vesicle Glycoprotein 2A in the Brain. Journal of Nuclear Medicine, 2016, 57, 777-784.	5.0	197
126	Increased Nanoparticle Delivery to Brain Tumors by Autocatalytic Priming for Improved Treatment and Imaging. ACS Nano, 2016, 10, 4209-4218.	14.6	103

#	Article	IF	CITATIONS
127	PET imaging evaluation of [18F]DBT-10, a novel radioligand specific to α7 nicotinic acetylcholine receptors, in nonhuman primates. European Journal of Nuclear Medicine and Molecular Imaging, 2016, 43, 537-547.	6.4	20
128	Effects of Jitai Tablet, A Traditional Chinese Medicine, on Spontaneous Withdrawal Symptoms and Modulation of Dopaminergic Functions in Morphine-Dependent Rats. Phytotherapy Research, 2015, 29, 687-694.	5.8	8
129	A Promising PET Tracer for Imaging of α7 Nicotinic Acetylcholine Receptors in the Brain: Design, Synthesis, and in Vivo Evaluation of a Dibenzothiophene-Based Radioligand. Molecules, 2015, 20, 18387-18421.	3.8	13
130	Test–Retest Reproducibility of Binding Parameters in Humans with <sup>11</sup> C-LY2795050, an Antagonist PET Radiotracer for the κ Opioid Receptor. Journal of Nuclear Medicine, 2015, 56, 243-248.	5.0	35
131	Deficits in Prefrontal Cortical and Extrastriatal Dopamine Release in Schizophrenia. JAMA Psychiatry, 2015, 72, 316.	11.0	304
132	Evaluation of [ 18 F]-(-)-norchlorofluorohomoepibatidine ([ 18 F]-(-)-NCFHEB) as a PET radioligand to image the nicotinic acetylcholine receptors in non-human primates. Nuclear Medicine and Biology, 2015, 42, 570-577.	0.6	17
133	Synthesis of [ 18 F]FMISO in a flow-through microfluidic reactor: Development and clinical application. Nuclear Medicine and Biology, 2015, 42, 578-584.	0.6	19
134	Imaging human brown adipose tissue under room temperature conditions with 11C-MRB, a selective norepinephrine transporter PET ligand. Metabolism: Clinical and Experimental, 2015, 64, 747-755.	3.4	25
135	Imaging robust microglial activation after lipopolysaccharide administration in humans with PET. Proceedings of the National Academy of Sciences of the United States of America, 2015, 112, 12468-12473.	7.1	265
136	Measurement of <i>B</i> <sub>max</sub> and <i>K</i> <sub>d</sub> with the Glycine Transporter 1 Radiotracer <sup>18</sup> F-MK6577 using a Novel Multi-Infusion Paradigm. Journal of Cerebral Blood Flow and Metabolism, 2015, 35, 2001-2009.	4.3	10
137	Imaging the Cannabinoid CB1 Receptor in Humans with [ <sup>11</sup> C] OMAR: Assessment of Kinetic Analysis Methods, Test–Retest Reproducibility, and Gender Differences. Journal of Cerebral Blood Flow and Metabolism, 2015, 35, 1313-1322.	4.3	79
138	Longitudinal changes of dopamine transporters in heroin users during abstinence. Psychopharmacology, 2015, 232, 3391-3401.	3.1	10
139	Neuroprotective Effects of Jitai Tablet, a Traditional Chinese Medicine, on the MPTP-Induced Acute Model of Parkinson's Disease: Involvement of the Dopamine System. Evidence-based Complementary and Alternative Medicine, 2014, 2014, 1-9.	1.2	15
140	Association of In Vivo κ-Opioid Receptor Availability and the Transdiagnostic Dimensional Expression of Trauma-Related Psychopathology. JAMA Psychiatry, 2014, 71, 1262.	11.0	67
141	Imaging Nicotine- and Amphetamine-Induced Dopamine Release in Rhesus Monkeys with [11C]PHNO vs [11C]raclopride PET. Neuropsychopharmacology, 2014, 39, 866-874.	5.4	43
142	Kinetic Modeling of 11C-LY2795050, A Novel Antagonist Radiotracer for PET Imaging of the Kappa Opioid Receptor in Humans. Journal of Cerebral Blood Flow and Metabolism, 2014, 34, 1818-1825.	4.3	42
143	An Improved Antagonist Radiotracer for the $\hat{I}^e$ -Opioid Receptor: Synthesis and Characterization of 11C-LY2459989. Journal of Nuclear Medicine, 2014, 55, 1185-1191.	5.0	26
144	Synthesis and evaluation of a 18F-labeled spirocyclic piperidine derivative as promising $If1$ receptor imaging agent. Bioorganic and Medicinal Chemistry, 2014, 22, 5270-5278.	3.0	17

#	Article	IF	CITATIONS
145	Preparation of the metabotropic glutamate receptor 5 (mGluR5) PET tracer [ 18 F]FPEB for human use: An automated radiosynthesis and a novel one-pot synthesis of its radiolabeling precursor. Applied Radiation and Isotopes, 2014, 94, 349-354.	1.5	23
146	Imaging Glutamate Homeostasis in Cocaine Addiction with the Metabotropic Glutamate Receptor 5 Positron Emission Tomography Radiotracer [11C]ABP688 and Magnetic Resonance Spectroscopy. Biological Psychiatry, 2014, 75, 165-171.	1.3	66
147	Reductions in Brain 5-HT1B Receptor Availability in Primarily Cocaine-Dependent Humans. Biological Psychiatry, 2014, 76, 816-822.	1.3	50
148	Parametric Imaging and Test–Retest Variability of <sup>11</sup> C-(+)-PHNO Binding to D <sub>2</sub> /D <sub>3</sub> Dopamine Receptors in Humans on the High-Resolution Research Tomograph PET Scanner. Journal of Nuclear Medicine, 2014, 55, 960-966.	5.0	38
149	Evaluation of the agonist PET radioligand [11C]GR103545 to image kappa opioid receptor in humans: Kinetic model selection, test–retest reproducibility and receptor occupancy by the antagonist PF-04455242. NeuroImage, 2014, 99, 69-79.	4.2	54
150	Quantitative Analysis of [11C]-Erlotinib PET Demonstrates Specific Binding for Activating Mutations of the EGFR Kinase Domain. Neoplasia, 2013, 15, 1347-1353.	5.3	43
151	Synthesis and Evaluation of 11C-LY2795050 as a κ-Opioid Receptor Antagonist Radiotracer for PET Imaging. Journal of Nuclear Medicine, 2013, 54, 455-463.	5.0	80
152	Tracer Kinetic Modeling of [ <sup>11</sup> C]AFM, a New PET Imaging Agent for the Serotonin Transporter. Journal of Cerebral Blood Flow and Metabolism, 2013, 33, 1886-1896.	4.3	17
153	Determination of In Vivo <i>B</i> <sub>max</sub> and <i>K</i> <sub>d</sub> for <sup>11</sup> C-GR103545, an Agonist PET Tracer for κ-Opioid Receptors: A Study in Nonhuman Primates. Journal of Nuclear Medicine, 2013, 54, 600-608.	5.0	31
154	In Vivo Imaging of the Metabotropic Glutamate Receptor 1 (mGluR1) with Positron Emission Tomography: Recent Advance and Perspective. Current Medicinal Chemistry, 2013, 21, 113-123.	2.4	34
155	Synthesis and characterization of two pet radioligands for the metabotropic glutamate 1 (mGlu1) receptor. Synapse, 2012, 66, 1002-1014.	1.2	9
156	Reduced Amygdala Serotonin Transporter Binding in Posttraumatic Stress Disorder. Biological Psychiatry, 2011, 70, 1033-1038.	1.3	79
157	Recovery from chronic spinal cord contusion after nogo receptor intervention. Annals of Neurology, 2011, 70, 805-821.	5.3	87
158	Development of Effective PET and SPECT Imaging Agents for the Serotonin Transporter: Has a Twenty-Year Journey Reached its Destination?. Current Topics in Medicinal Chemistry, 2010, 10, 1499-1526.	2.1	39
159	High-resolution imaging of brain 5-HT1B receptors in the rhesus monkey using [11C]P943. Nuclear Medicine and Biology, 2010, 37, 205-214.	0.6	40
160	Enhanced selective serotonin re-uptake inhibitors as antidepressants: 2004 – 2006. Expert Opinion on Therapeutic Patents, 2007, 17, 889-907.	5.0	11
161	Epibatidine analogues as selective ligands for the αxβ2-containing subtypes of nicotinic acetylcholine receptors. Bioorganic and Medicinal Chemistry Letters, 2005, 15, 4385-4388.	2.2	21
162	Synthesis of potent and selective serotonin 5-HT1B receptor ligands. Bioorganic and Medicinal Chemistry Letters, 2005, 15, 4786-4789.	2.2	11

#	Article	IF	CITATIONS
163	Fluorinated Diaryl Sulfides as Serotonin Transporter Ligands:Â Synthesis, Structureâ^'Activity Relationship Study, and in Vivo Evaluation of Fluorine-18-Labeled Compounds as PET Imaging Agents. Journal of Medicinal Chemistry, 2005, 48, 2559-2570.	6.4	59
164	A Positron Emission Tomography Radioligand for the in Vivo Labeling of Metabotropic Glutamate 1 Receptor:Â (3-Ethyl-2-[11C]methyl-6-quinolinyl)(cis- 4-methoxycyclohexyl)methanone. Journal of Medicinal Chemistry, 2005, 48, 5096-5099.	6.4	52
165	11C-GR103545, a radiotracer for imaging kappa-opioid receptors in vivo with PET: synthesis and evaluation in baboons. Journal of Nuclear Medicine, 2005, 46, 484-94.	5.0	59
166	In vivo affinity of [18F]fallypride for striatal and extrastriatal dopamine D2 receptors in nonhuman primates. Psychopharmacology, 2004, 175, 274-286.	3.1	63
167	A new positron emission tomography imaging agent for the serotonin transporter: synthesis, pharmacological characterization, and kinetic analysis of [11C]2-[2-(dimethylaminomethyl)phenylthio]-5-fluoromethylphenylamine ([11C]AFM). Nuclear Medicine and Biology, 2004, 31, 543-556.	0.6	38
168	A PET imaging agent with fast kinetics: synthesis and in vivo evaluation of the serotonin transporter and Biology, 2004, 31, 727-738.	0.6	22
169	The new PET imaging agent [11C]AFE is a selective serotonin transporter ligand with fast brain uptake kinetics. Nuclear Medicine and Biology, 2004, 31, 983-994.	0.6	20
170	Comparative evaluation of serotonin transporter radioligands 11C-DASB and 11C-McN 5652 in healthy humans. Journal of Nuclear Medicine, 2004, 45, 682-94.	5.0	114
171	Relationships between radiotracer properties and image quality in molecular imaging of the brain with positron emission tomography. Molecular Imaging and Biology, 2003, 5, 363-375.	2.6	202
172	Synthesis and pharmacological characterization of a new PET ligand for the serotonin transporter: [11C]5-bromo-2-[2-(dimethylaminomethylphenylsulfanyl)]phenylamine ([11C]DAPA). Nuclear Medicine and Biology, 2002, 29, 741-751.	0.6	23
173	Comparative Evaluation in Nonhuman Primates of Five PET Radiotracers for Imaging the Serotonin Transporters: [ <sup>11</sup> C]McN 5652, [ <sup>11</sup> C]ADAM, [ <sup>11</sup> C]DASB, [ <sup>11</sup> C]DAPA, and [ <sup>11</sup> C]AFM. Journal of Cerebral Blood Flow and Metabolism, 2002, 22, 1377-1398.	4.3	111